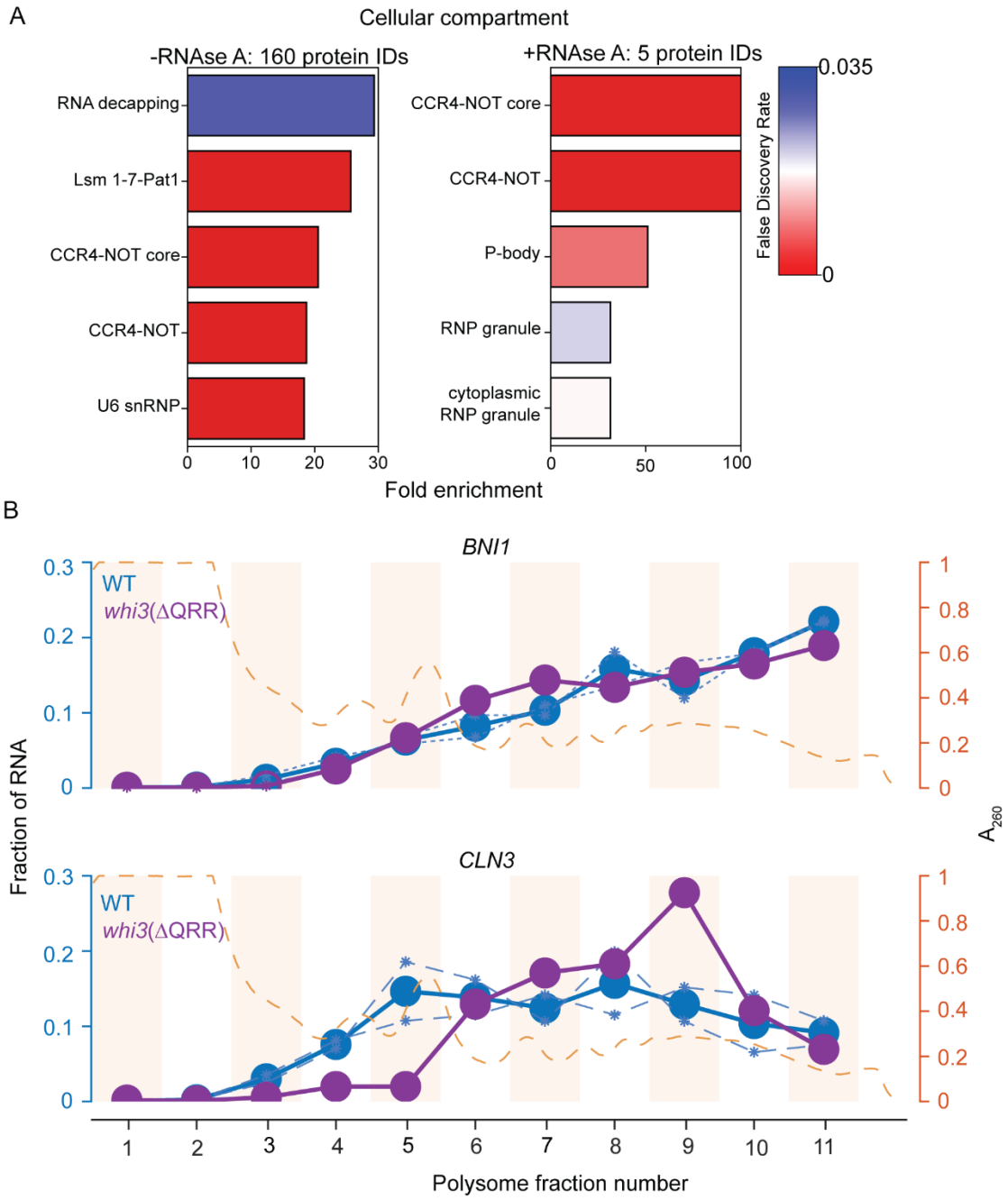

Figure S1, related to Figure 2 and 3. Whi3 condensates show enrichment of translation regulators.

A. Bar plots showing top five enriched GO terms for cellular compartments associated with Whi3 condensates in RNA intact (-RNAseA) or RNA-degraded (+RNAse A) *Ashbya* lysates.

B. Polysome profile of CLN3 and BNI1 in WT and deltaQRR indicates that these RNAs are polysome associated in WT, and CLN3 shows a loss of a non-translating pool in deltaQRR n= 2 independent sucrose gradients.

Protein ID	Log_2(FC)	RNAse A treatment	Class
Q75EE7	1.54	-	Translation
Q754R9	1.58	-	Translation
Q759L9	1.61	-	Translation
Q75C13	1.51	-	Translation
Q75AT6	1.62	-	Translation
Q759A5	1.56	-	Translation
Q757D7	1.66	-	Translation
Q75AK5	1.74	-	Translation
Q751I7	1.58	-	Translation
Q754V6	1.57	-	Translation
Q754C5	1.63	-	Translation
Q751Y7	1.68	-	Translation
Q754N8	1.62	-	Translation
Q75F39	1.52	-	Translation
Q75CK1	1.68	-	Translation
Q75F00	1.5	-	Decay
Q75BI3	2.52 & 1.75	-/+	Decay
Q75BK1	2.24	-	Decay
Q75BD0	2.25 & 1.67	-/+	Decay
Q75DA5	2.56	-	Decay
Q758F6	2.41	-	Decay

Table S1, related to Figure 2. Whi3 interactors involved in RNA translation and metabolism.

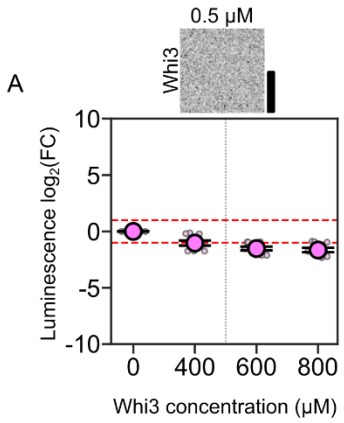

Figure S2, related to figure 4. Translation of *CLN3-Nluc* mRNA is repressed even in the absence of Whi3 condensates.

A. Translation of CLN3-Nluc reporter RNA as a function of Whi3 concentration. Luminescence values are displayed as log_2(FC) over RNA-only conditions. Measurements are taken from at least three separate RR lysates with three technical replicates per lysate (see Methods). Fluorescence image shows Whi3 signal at 0.5 µM. Scale bar = 2.5 µm.

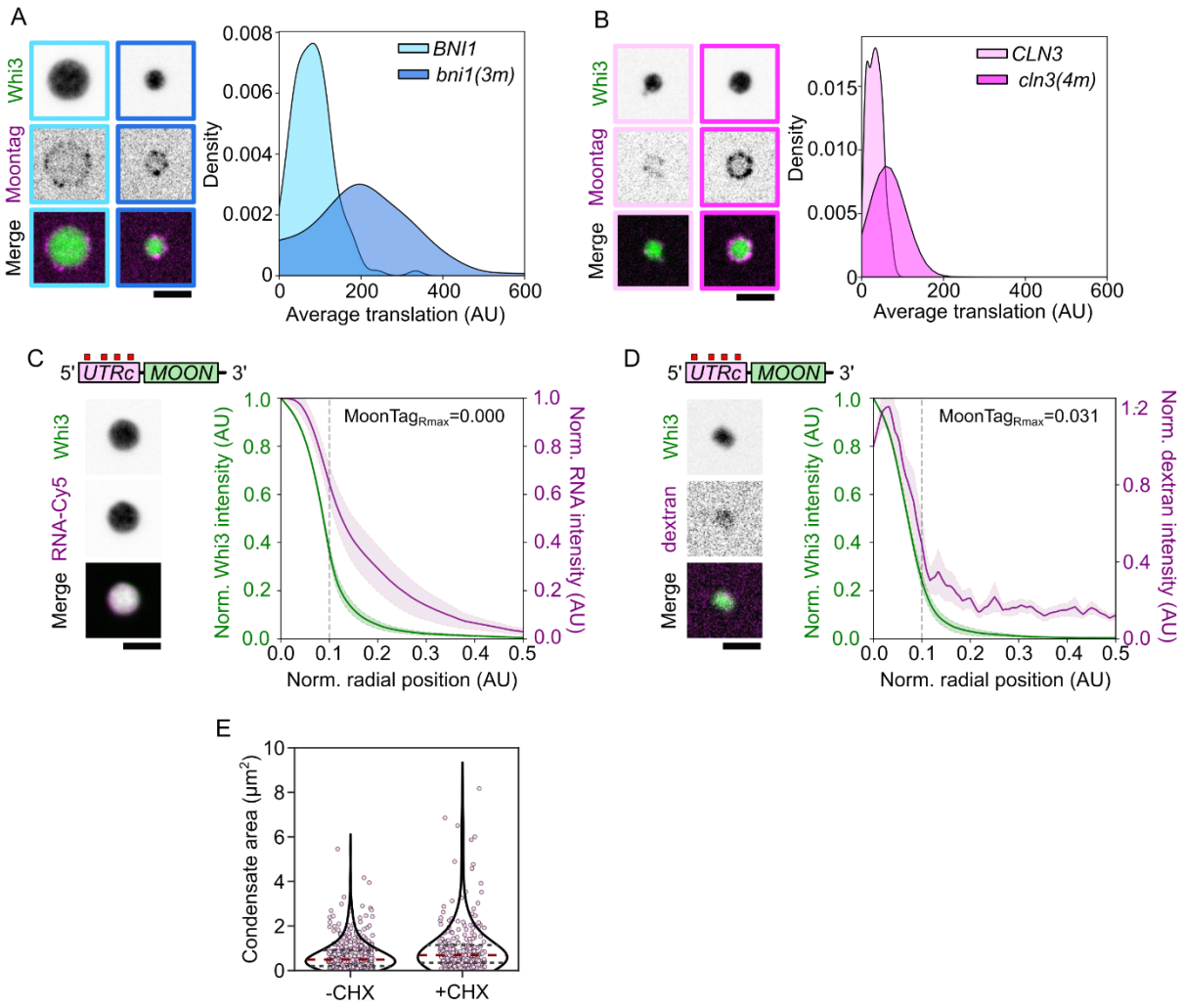

Figure S3, related to figure 5. Translation of mRNA, but not RNA or dextran, is enriched at the Whi3 condensate interface.

A. Fluorescence image of a Whi3 condensate formed with *bni1(3m)-Moon* showing translation of mRNAs on the surface. Kernal density estimate of probability density of the average translation signal associated with condensates formed with either *BNI1-Moon* (light-blue; n=299) or *bni1(3m)-Moon* (dark blue; n=262).

B. Fluorescence image of a Whi3 condensate formed with *cln3(4m)-Moon* showing translation of mRNAs on the surface. Kernal density estimate of the probability density of the average translation signal associated with condensates formed with *CLN3-Moon* (light-pink; n=299) or *cln3(4m)-Moon* (dark-pink; n=460).

C. Fluorescence images of Whi3 condensates formed with *Cy5-CLN3-Moon*. Radial intensity profile of Whi3 condensates formed with *Cy5-CLN3-Moon*, showing fluorescence intensity as a function of radial position in the condensate for Whi3 and Cy5-RNA. The condensate periphery, grey line, is approximately 0.1 AU from the center of the condensate. The radial position associated with the maximum MoonTag intensity recorded, MoonTagRmax, is shown. Trace shows the average intensity of 55 condensates ± SEM. Scale bar = 2.5 μm.

D. Fluorescence images of Whi3 condensates formed with CLN3-Moon in the presence of 10K MW dextran-rhodamine. Radial intensity profile of Whi3 condensates formed with CLN3-Moon, showing fluorescence intensity as a function of radial position in the condensate for Whi3 and dextran. The condensate periphery, grey line, is approximately 0.1 AU from the center of the condensate. The radial position associated with the maximum MoonTag intensity recorded, MoonTagRmax, is shown. Trace shows the average intensity of 33 condensates ± SEM. Scale bar = 2.5 μm.

E. Whi3 condensate area for *CLN3-Moon* condensates in the translation competent RR lysates (CHX-; 435) or translation inhibited RR lysates (CHX+; n=255). Individual dots indicate a single condensate.

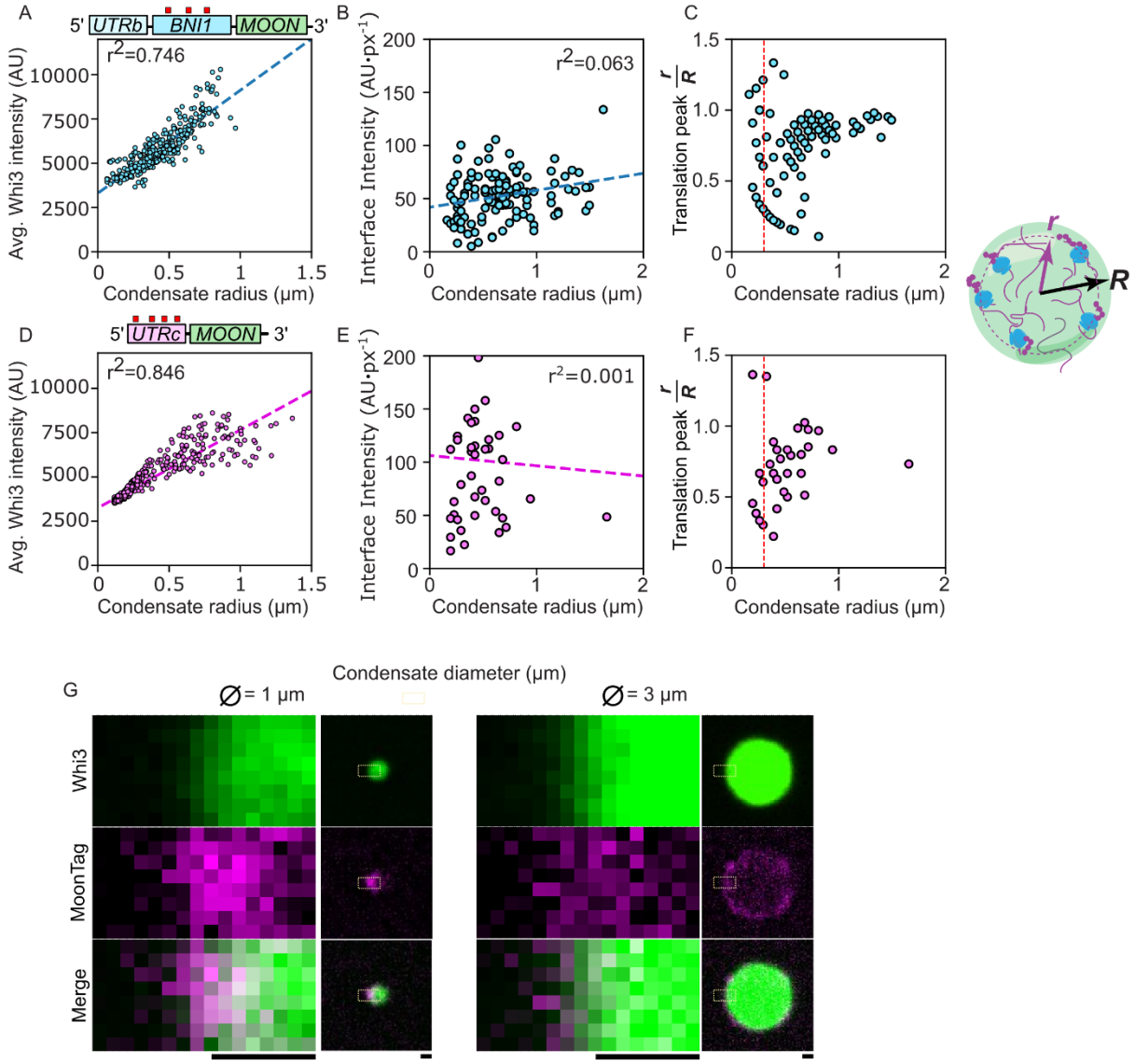

Figure S4, related to figure 5. Whi3 concentration and translation localization scale with condensate size.

A. Whi3 concentration as a function of condensate radius for Whi3 condensates formed with BNI1-Moon. Each individual dot represents a condensate (n=300).

B. Translation signal at the condensate interface per unit pixel, as a function of condensate radius for Whi3 condensates formed with BNI1-Moon. Each individual dot represents a condensate (n=123).

C. Location of the translation-enrichment zone in condensates formed with BNI1-Moon as a function of condensate radius. Location of the translation peak is expressed as the ratio of the translation peak (r) relative to the condensate periphery (R). Dashed red line represents indicates the resolution limit between the center and condensate periphery. Each individual dot represents a condensate (n=123).

D. Whi3 concentration as a function of condensate radius for Whi3 condensates formed with CLN3-Moon (n=854). Each individual dot represents a condensate.

E. Translation signal at the condensate interface per unit pixel, as a function of condensate radius for Whi3 condensates formed with CLN3-Moon. Each individual dot represents a condensate (n=42).

F. Location of the translation-enrichment zone in condensates formed with CLN3-Moon as a function of condensate radius. Location of the translation peak is expressed as the ratio of the translation peak (r) relative to the condensate periphery (R). Dashed red line represents indicates the resolution limit between the center and condensate periphery. Each individual dot represents a condensate (n=42).

G. 2D-fluorescence image representing the condensate interface for small (ø=1) and large (ø=3) condensates formed with BNI1-Moon. Scale bar = 0.5 μm.

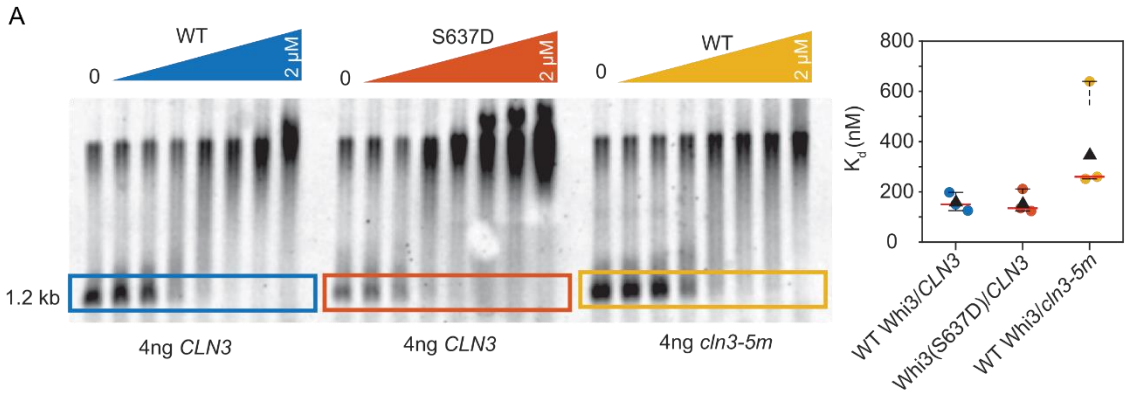

Figure S5, related to figure 5 and 6. Phospho-state impacts Whi3 target translation independently of binding site affinity

A. Apparent dissociation constants for WT or 0xWBS Cln3 RNA with WT or S637D Whi3 from EMSAs. Three technical replicates of WTWhi3/WT cln3, S637D Whi3/WT CLN3 and WT Whi3/Cln3 0xWBS shows that S637D does not severely change Kd, relative to WT, whereas WT Whi3 shows decreased affinity for the RNA variant with no binding sites.